JOURNAL OF MATERIALS SCIENCE 31 (1996) 5859–5864

The visualization of water transport through hydrophobic polymer coatings applied to building sandstones by broad line magnetic resonance imaging

A.J. BOHRIS, P.J. McDONALD, M. MULHERON*
*Departments of Physics and *Civil Engineering, University of Surrey, Guildford, Surrey, GU2 5XH UK*

It is shown that broad line gradient echo magnetic resonance imaging is an ideal tool with which to study the ingress of hydrophobic polymer surface treatments into porous building materials, specifically in this case sandstone. It is further shown that the method can be used to quantitatively visualize the movement of water into and through the treated material, both from the surface and bulk, as a function of time. The influence of treatment cure time, cure temperature and substrate hydration on the subsequent water transport have been investigated. For the first time direct evidence of water pumping through a treated surface is presented.

1. Introduction

Degradation of ceramic building materials such as stone, brick, concrete and other cement based mortars is often related to the presence of liquid water within the capillary pore structure of the material. For degradation which is physical in nature, for example that resulting from freeze–thaw cycling under water saturated conditions, or which is the result of chemical action, such as sulphate attack, the mere presence of water in the capillary pores is sufficient for the degradation to occur. In other instances the movement of liquid is important. For instance, environmental water moving into the pore system carries with it aggressive ions such as chloride which enable deterioration of not only the ceramic but also of companion materials such as steel reinforcement in concrete. Alternatively, in large-scale engineering structures, damage can occur when water saturated with salts moves from the bulk of the material to the surface and evaporates leaving behind a surface build-up of salt products. As a consequence, the control of water transport into and out of porous building materials is of major economic concern. Considerable effort has been expended in developing surface coatings which can be applied to engineering structures with the aim of reducing subsequent water ingress. An important, and necessary, property of these coatings is that while restricting the uptake of liquid water into the bulk they should not restrict the evaporation of water out of the underlying material. This ensures that a high humidity environment, which can cause damage to both the coating and the near surface layers does not build-up behind the coating. It also helps the structure to gradually dry out reducing the long-term opportunities for physical and chemical attack to occur.

In recent years the application of hydrophobic surface treatments in particular has been popular as a means of inhibiting water ingress. Indeed some regulatory authorities in the UK now specify their application on newly constructed reinforced concrete structures as a matter of course [1]. Typically, these coatings penetrate some 2–50 mm into the surface. When they are properly cured, they reduce the wettability of the surface and encourage the run-off of rain water from vertical surfaces, without significantly changing either the colour or appearance of the parent material. However, it has been reported by various bodies involved in the preservation of historic stone and brick structures that in some cases hydrophobic coatings are at best ineffective and at worst actively encourage deterioration [2]. In consequence they do not allow the indiscriminate use of coatings.

The difference of opinion, and experience as regards the use of hydrophobic coatings reflects the range of building materials that have been treated, the range of available treatments and the range of water related deterioration mechanisms. In order to make informed judgments on the use of coatings for any specific case, it is first necessary to understand the dynamics of the treatment uptake by the substrate and secondly to quantify the effect of the treatment on water transport into, out of and through the bulk of the material. Established methods for obtaining this information are based on measurements of the change in surface characteristics of the treated material and include volumetric surface absorption techniques [3], gravimetric analysis [4], contact angle [5] and electrical conductivity [6]. These, and other techniques, are fundamentally limited by their inability to obtain depth-profile information as a function of time without

0022–2461

destroying the material under test. Repeated depth-profile measurements on the same sample are thus impossible so that time course studies cannot be undertaken. A more fundamental limitation of all these approaches is that they do not clearly distinguish between bound and mobile states of water.

Magnetic resonance imaging, (MRI), is a very powerful technique for mapping hydrogen (water) distribution and dynamics in many systems. Derived from nuclear magnetic resonance, (NMR), MRI was originally developed for *in vivo* medical applications but in recent years has found increasing application in non-medical fields, particularly in the petroleum, chemicals and food processing industries [7]. MRI is non-destructive and chemically and physically non-invasive. It can provide spatially resolved maps of the distribution of water and other small organic molecules, usually in solution in porous media. The spatial resolution for materials applications is typically sub-millimetre. Contrast between bound and mobile fluids is usually obtained on the basis of their different spin–spin relaxation times, T_2. This time constant, which can range from microseconds in rigid solids, to seconds in bulk pure liquids, is intimately related to molecular motion. Mobile liquids invariably have much longer relaxation times than confined or bound liquids.

NMR and MRI have already been applied to cementitious systems by a number of authors [8, 9, 10]. However, in many early MRI studies it has been realised that the quantitative information which can be extracted and the image quality is severely limited. This is due to three factors which reduce the spin–spin relaxation time of water hydrogen in cements to values of order or substantially below 1 ms which is the lower limit measurement threshold for most conventional scanners operating with liquid state techniques. The first relaxation mechanism is paramagnetic impurities, the second is water self-diffusion through magnetic susceptibility field gradients in the vicinity of pore surfaces and the third is the binding of water molecules to pore surface sites. Amongst other systems relevant to the current study, MRI has also been widely applied to oil and gas reservoir sandstones. Indeed the petroleum engineering industry, widely concerned with porous rock, was one of the first outside medicine to widely exploit MRI, [11, 12, 13]. None the less, similar relaxation time limitations are known to apply and in consequence most work has been carried out at high saturation levels and in cleaned stones.

There are a number of MRI techniques, collectively known as broad line techniques, now being developed and applied which are specifically designed to overcome the limitations of short spin–spin relaxation times. Although these more specialist methods are unable to offer the wealth of relaxation contrast parameters of some of the conventional liquid state methods, in general they do permit quantitative mapping of density and relaxation times. Reviews of broad line MRI have been presented by a number of authors [14, 15]. In a recent letter, [16], some of the authors demonstrated the considerable power of one emerging broad line MRI method, stray field imaging, to follow the ingress of a surface hydrophobic polymer treatment into a cement based mortar sample and subsequently to visualize the movement of water into the same sample as a function of time. The profiles presented clearly showed the depth penetration of the treatment and how it inhibited forward water uptake from the treated surface. Nunes *et al.* have also used stray field imaging to monitor the cure of cement pastes [17]. In this more detailed follow-up study to our own work, we follow the ingress of another coating and more specifically measure its effectiveness in controlling water transport through the surface layer in both the forward and reverse directions for a variety of treatment cure conditions. Since the preliminary work was complicated by the on-going cure exhibited by the cement based sample during the experiment, which caused the capillary pore system to change with time, building sandstone samples in which the capillary pore structure is known to be substantially unchanging have been used in this work. Moreover, instead of stray field imaging, broad line gradient echo imaging has been used. We have previously shown that this technique is particularly suited to providing detailed quantitative information about water transport, motion and distribution in gas reservoir sandstones at low saturation levels [18].

2. Methodology

The gradient echo method has been extensively discussed elsewhere [19, 20]. Here we give only a very brief overview of the technique. A continuously oscillating magnetic field gradient is applied across the sample in the direction to be profiled. A radio frequency pulse is applied at a gradient zero crossing and the NMR signal in the form of a gradient echo recorded one gradient cycle later. The echo is linearized to take account of the time-dependent gradient and then Fourier transformed to yield a profile in the gradient direction. For sufficiently small gradient period and hence echo time, the profile so produced is proportional to the hydrogen density in the sample, assuming a ^{1}H experiment. A useful variation to the experiment carried out here and based on the classic Carr–Purcell–Meiboom–Gill (CPMG) sequence [19, 21], is to apply 180° pulses at alternate gradient nodes after the initial first pulse and to collect echoes at the intermediate nodes. Multiple echoes recorded in this way yield a series of true T_2 weighted profiles. The intensities of profiles calculated from such series of echoes can be fitted at each location to exponential decay functions to yield a measure of the local T_2 and also, by back extrapolation of the decays to the origin, a better estimate of the local hydrogen density.

Throughout the work described here the multiple echo T_2 technique has been employed. The gradient period is 216 μs and the gradient amplitude 30 G/cm. The 90° pulse length is 8.3 μs and four CPMG echoes have been recorded. Typically 100 averages were acquired with a repetition time of 1 s. The ^{1}H NMR frequency was 30 MHz. The samples were cylindrical in shape, 24 mm in diameter and approximately

20 mm long, and were cut from a large block of as excavated green sandstone using a water-cooled diamond coring drill. All the samples were first equilibrated over several days in a 50% humidity environment at 20 °C. Once equilibrated they were treated on one end by the application of 0.2 ml of a solution of 5% alkyl methoxy silane in methanol. After this they were stored and profiled as discussed below. In most instances a rubber test sample has been imaged immediately prior to the sample of interest in order to yield a standard which allows quantitative comparison of images acquired periodically over long time periods.

The pore size distribution and porosity of the sandstone have been previously characterized using mercury intrusion porosimetry, helium autopycnometry and gravimetric methods [22]. This analysis has shown that the sandstone has a typical total porosity of 25% and a mean pore diameter of 5 μm with over 90% of the pores being greater than 1 μm. The performance of silane-based hydrophobic treatments applied to this sandstone has also been studied using conventional engineering measurement techniques including contact angle, volumetric water absorption (Karsten tube) and electrical conductivity. The treatment analysis has only been able to show that the fully cured treatment is effective at inhibiting absorption of water droplets applied to the sandstone surface in the short term.

3. Results and discussion

Fig. 1 shows a series of profiles recorded from a sample of untreated sandstone initially equilibrated at 50% relative humidity as a function of time after one end of the core was placed in a shallow (2 mm) water bath. This bath simulated an infinite supply of water in direct physical contact with the sandstone. The profiles show the rapid transport of bulk water through the capillary pore system in the vertical direction. The water has reached the top of the core in less

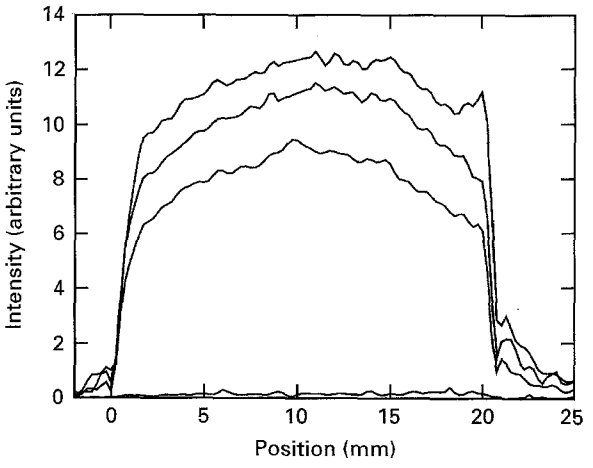

Figure 1 Profiles recorded from an untreated sample of green sandstone. The sample extends from 0 to 21 mm on the scale. Water ingress is from the right. The profiles shown were recorded (from bottom to top) immediately prior to water exposure and after 0.5 h, 1 day and 2 days.

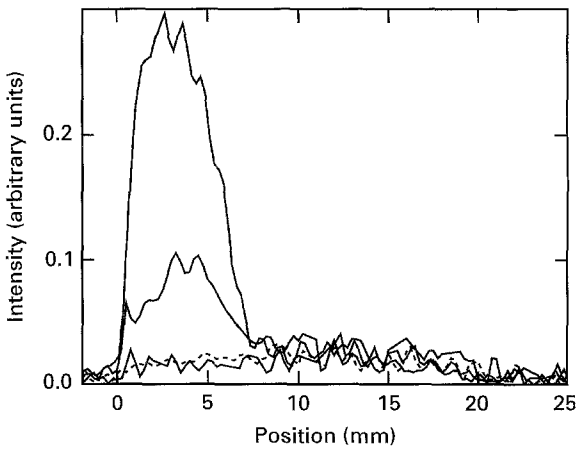

Figure 2 Profiles showing the ingress, cure and drying of alkoxysilane treatment applied to the left side of a sandstone sample. The sample extends from 0 to 20 mm. The profiles are recorded before treatment (dashed line) and (from top) 12 min, 80 min and 18 days after treatment.

than 0.5 h, with an essentially uniform water saturation being seen. Continued immersion does not greatly increase the water uptake. After 2 days the sample had absorbed 9% weight of water compared to the sample mass after equilibration at 50% relative humidity.

Fig. 2 shows the results of an experiment to monitor the ingress of the siloxane treatment into a second sample. The first profile, recorded 12 min after the treatment application clearly shows that the treatment has penetrated to a depth of 6.5 ± 1.0 mm. Subsequent profiles show a loss of signal intensity but no further treatment ingress. The loss of signal intensity is partly due to solvent evaporation. It is also due to a shortening below the echo time of the experiment of the spin–spin relaxation time of the remaining treatment as it becomes immobilised. Thus the treatment becomes "invisible" to the imaging method after a few hours. However, it can be seen using the alternative technique of stray field imaging which operates with a much smaller echo time, as we have previously shown. After 3 days the sample exhibited short term inhibition of water measured by droplet contact angle, as expected from previous studies. This experiment was repeated three times and the depth of solvent ingress was shown to be remarkably constant, 7 ± 1 mm.

In order to assess the effectiveness of the treatment by NMR means, a series of samples were treated as above and cured under a variety of conditions. They were subsequently exposed to a shallow water bath from the untreated end. Fig. 3 shows profiles recorded from a sample in which the curing consisted of leaving the sample at room temperature for 4 days at 50% relative humidity and for which a water drop on the treated surface indicated that the treatment was active. However, the NMR profiling shows rapid initial uptake of water throughout the whole core with only a very slight retardation of water ingress in the treated region. This retardation is evidenced by the water concentration profiles after typically 1.5 h at about 8.5 mm. After 24 h, the profile bears direct comparison with those in Fig. 1 and is as if there were no treatment

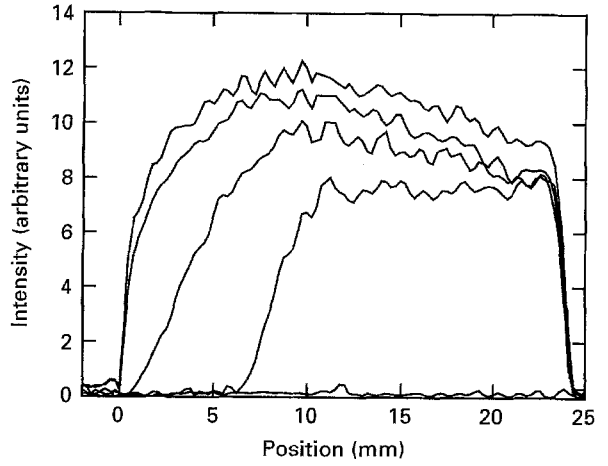

Figure 3 Profiles showing the uptake of water into the untreated end (right-hand side) of a treated sample. The treatment cure was for 4 days at room temperature. The profiles were recorded (from bottom to top) immediately prior to water exposure and after 1.5 h, 6 h, 1 day and 3 days.

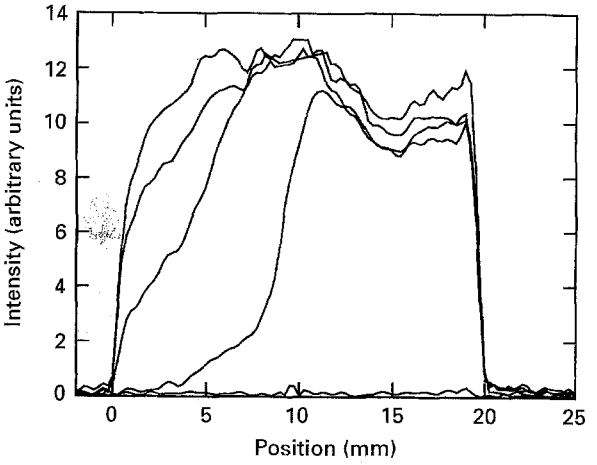

Figure 5 Profiles showing the uptake of water into the untreated end (right-hand side) of a treated sample. The treatment cure was for 42 days at room temperature. The profiles were recorded (from bottom to top) immediately prior to water exposure and after 1.0, 6.0, 12 h and 2 days.

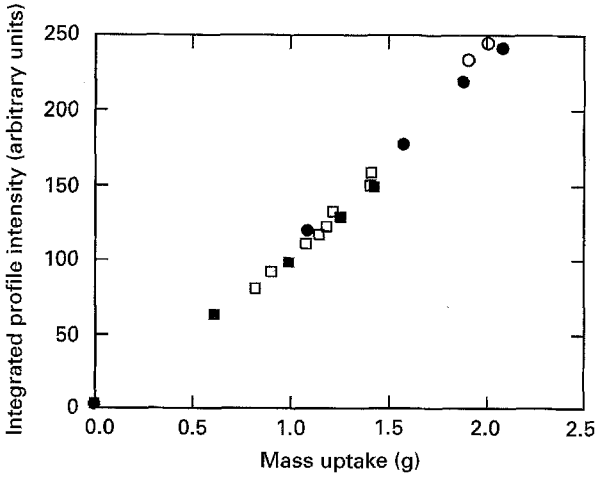

Figure 4 The figure shows the correlation between profile integrated intensity and mass uptake for the same sample as shown in Figs 3 (circles) and 7 (squares). In each case the correlation is linear and the solid symbols refer to the profiles shown whereas the open symbols refer to other profiles not shown in the other figures.

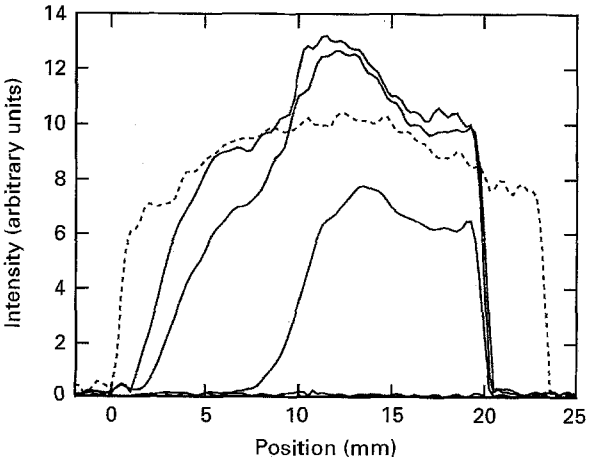

Figure 6 Profiles showing the uptake of water into the untreated end (right-hand side) of a treated sample. The treatment cure was for 3 days at 50 °C. The profiles were recorded (from bottom to top) immediately prior to water exposure and after 1 h, 1 day and 5 days. By way of comparison, the dashed profile shows water uptake after 1 h into an untreated sample stored at 50 °C for 3 days.

at all. In order to verify the quantification of the MRI water ingress measurements, the area of the profiles in Fig. 3 has been correlated with the sample mass increase. This correlation is shown in Fig. 4 from which it is seen that, to a very good approximation, the signal intensity in the profiles is directly proportional to the local water content. This emphasizes the quantitative nature of the broad line MRI method.

In order to investigate further, similar samples were treated and profiled as above except that the treatment was allowed to cure at room temperature for longer periods of 18, 28 and 42 days prior to immersion of the untreated end in the water bath. In each case the treated end was shown by contact angle testing to be hydrophobed. However, the water was found to pass right through the sample, in the reverse direction, in only a few hours by MRI. Profiles from the sample cured for 42 days are shown in Fig. 5. In each case there was again an excellent correlation between the integrated water intensity profile and mass uptake.

Since the treatment was seemingly not operating against reverse water transport for samples cured at room temperature, a sample was treated and directly cured at 50 °C for 3 days in an attempt to improve the action of the silane. This curing regime clearly improves the short-term inhibition of water transport through the capillary pore system of the treated material, as seen in Fig. 6. This figure shows profiles recorded prior to immersion of the untreated sample end in water and then after 1 h and 1 and 5 days. A sharp water concentration front is seen at 10 ± 1 mm in the profile recorded after 1 h and also in the later profiles. This corresponds to the inner treatment surface. In the longer term, the presence of the treatment is unable to prevent the passage of bulk water. In order to check that the water transport was unaffected by the sandstone being left at 50 °C for 3 days, an identical experiment was also carried out on an untreated sample. A profile recorded from this sample after 1 h of exposure to water is shown by the dashed line in Fig. 6.

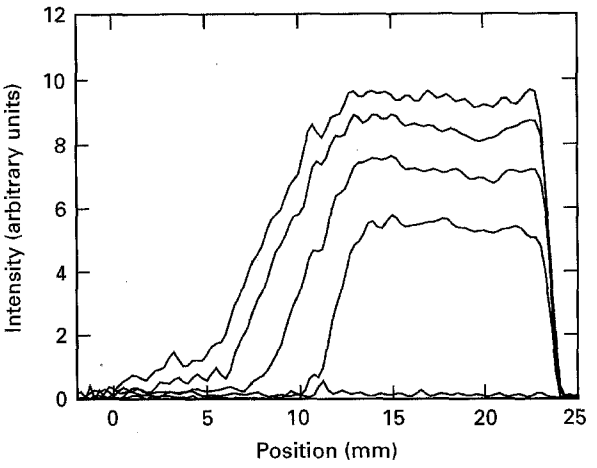

Figure 7 Profiles showing the uptake of water into the untreated end (right-hand side) of a treated sample. The treatment cure was for 4 days at room temperature followed by water saturation and then 3 days at 50 °C. The profiles were recorded (from bottom to top) immediately prior to the second exposure to water and after 1.0 h and 1, 7 and 28 days.

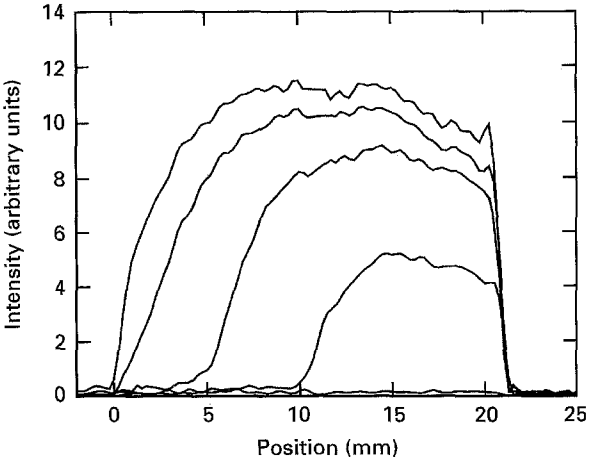

Figure 8 Profiles showing the uptake of water into the untreated end (right-hand side) of a treated sample. The treatment cure was for 4 days at room temperature followed by water saturation and then 3 days at 35 °C. The profiles were recorded (from bottom to top) immediately prior to the second exposure to water and after 2.0 and 12 h and 1 and 2 days.

In the real world, it is likely that, although the sandstone will be exposed to higher temperatures in hot weather, it is equally likely that it will first get wet. Therefore, in order to assess the effectiveness of the treatment curing at high temperature after exposure to water, a further sample was prepared. This sample was allowed to cure at room temperature for 4 days and was then exposed to the water bath for 3 days. A hydrophobed surface and rapid water uptake, as previously observed, was confirmed. The sample was then placed in an oven at 50 °C for a further 3 days. After this time, the sample, which had, of course, dried out, was exposed once more to the water bath at the untreated end and periodically profiled. The results are shown in Fig. 7. Surprisingly, the treatment is found to be even more effective than under any of the earlier cure conditions. As seen in Fig. 7, a significant retardation of water uptake in the region of treated stone is still evident after 1 month.

In reality, high temperature curing at 50 °C is impractical, even in hot weather. However, curing at intermediate temperatures between 20 and 50 °C is realistic on the long timescale in hot weather. Therefore, the experiment just described with treatment, room temperature curing, water exposure, heating and further water exposure was repeated with the high temperature phase conducted at 35 °C. The profiles resulting from the last water uptake are shown in Fig. 8 and show an intermediate effect of the treatment, as one might expect, with the water taking just a few hours to reach the treated region and a few days to cross it.

In many instances the water transport is from the treated surface rather than the back of the treated region, as discussed so far. Two samples were treated as before. One was cured at room temperature for three days and the other at 50 °C for three days. Water was then applied to the treated end of each sample from a saturated sponge placed in direct contact with the sandstone surface. The profiles recorded from the sample cured at 50 °C are presented in Fig. 9 and

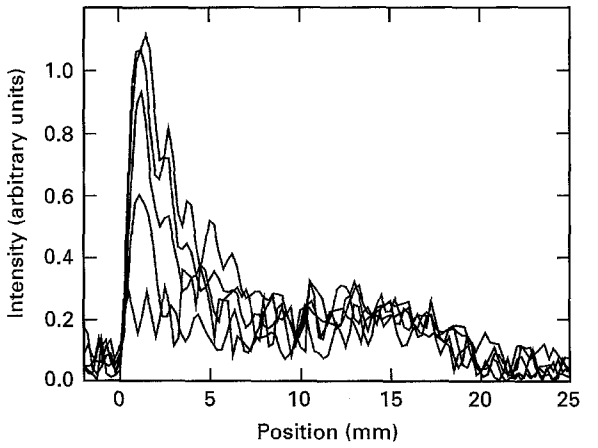

Figure 9 Profiles showing the uptake of water into the treated end (left-hand side) of a sample. The treatment cure was for 3 days at 50 °C. The profiles were recorded (from bottom to top) immediately prior to water exposure and after 0.5, 4 and 12 h and 2 days.

show a substantial hydrophobic effect with very little water transporting through the treated material in 2 days. The profiles recorded from the room temperature cured sample are shown in Fig. 10. They show a pronounced hydrophobic effect, but the profile shape requires some explanation. In the first few hours a water concentration gradient builds up across the treatment barrier from 0 to 10 mm and reaches the untreated sandstone beyond. Water concentration is thus able to build up in this untreated region, giving rise to the increased intensity in the profiles from 10 to 21 mm. As with all other studies, the mass uptake was correlated with the profile integral to check the quantification of the imaging procedure. This profile thus shows clear evidence of "water pumping" through a treated surface, a water transport and hence degradation mechanism, which has long been suspected but never before unambiguously demonstrated.

Throughout this work, multiple echo data has been acquired using the CPMG variant of the basic technique in an attempt to gain additional information about the water dynamics. However, for practical

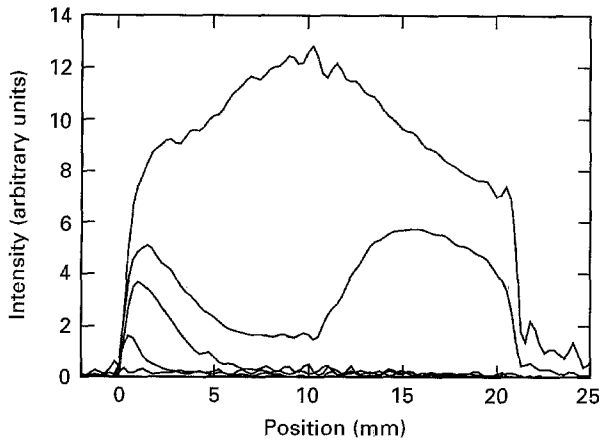

Figure 10 Profiles showing the uptake of water into the treated end (left-hand side) of a sample. The treatment cure was for 3 days at room temperature. The profiles were recorded (from bottom to top) immediately prior to water exposure and after 0.5, 4 and 12 h and 2 days.

reasons we have only been able to work with a maximum of four echoes acquired at $2 \times 216 = 432$ μs intervals. This number of echoes and echo spacing is inadequate to make more than the general comment that the spin–spin relaxation time decreases with water concentration. This is entirely as expected and fully consistent with previous work on reservoir rocks, where the so called fast diffusion model of relaxation has been shown to widely apply [23]. More quantitative analysis on the current sandstones requires either a much shorter pulse gap and commensurate increase in gradient strength or the use of a technique such as stray field imaging. Work in this area is going on.

4. Conclusions

In this paper, and our earlier letter, we have shown that broad line MRI is well able to map the transport of both water and polymer treatment into and through porous building materials. This has been done in time course experiments on the same sample and the results have been shown to be quantitatively reproducible and meaningful. Interpretation in terms of readily understood parameters has been achieved. Specifically related to sandstone, we have shown that the treatment applied in this work was ineffective if cure is at modest temperature for modest times. The treatment barrier efficiency was clearly demonstrated to increase with curing time and particularly temperature. It was also shown to be sensitive to the hydration state of the substrate at the time of cure. However, it has been shown that water will go through even well-cured treatment eventually. For the first time, clear and unambiguous evidence of "water pumping" from the surface of a stone sample, through the treatment surface layer and into dry stone beyond has been obtained. This has considerable implications for the durability of treated sandstones under freeze–thaw conditions. Whilst many of these conclusions have been suspected within the building industry for some considerable time, and whilst there has been consequent concern as to the cost effectiveness of applying these treatments as a matter of course, as now often required, this is the first time that a direct measurement procedure which can be used to assess treatments has been demonstrated.

Acknowledgements

AJB thanks the United Kingdom Engineering and Physical Science Research Council for a research studentship.

References

1. DEPARTMENT OF TRANSPORT, Specification BD 43/90 (HMSO, London, 1990).
2. SOCIETY FOR THE PROTECTION OF ANCIENT BUILDINGS TECHNICAL PANEL, "Colourless Water Repellant Surface Treatments" (Society for the Protection of Ancient Buildings, 1993).
3. RILEM Commision 25–PEM (Protection et Erosion des Monuments), *J. Mater. Struct.* **13** (1980) 175.
4. K. E-G. HASSAN and J. G. CABRERA, in Proceedings of the First International Symposium on Surface Treatment of Building Materials with Water Repellant Agents, Delft, November 1995, edited by F. H. Wittmann, T. A. J. M. Siemes, and L. G. W. Verhoef (University of Delft 1995) p. 33.
5. K. LITMANN, in Proceedings of the International Conference "ConChem", Karlsruhe, 1994, (ConChem 1994) p. 521.
6. D. WHITING, D. B. OST, M. NAGI and P. D. CADY, "Condition Evaluation of Concrete Bridges Relative to Reinforcement Corrosion, Vol 5: Methods for Evaluating the Effectiveness of Penetrating Sealers", Strategic Highway Research Program (US), SHRP-S/FR-92-107 (1992).
7. B. BLUMICH and W. KUHN (eds), in "Magnetic resonance microscopy: methods and application in materials science, agriculture and biomedicine" (VCH Publishers, New York, 1992).
8. W. P. HALPERIN, J. Y. JEHNG and Y. Q. SONG, *Magn. Reson. Imaging* **21** (1994) 169.
9. J. LINK, J. KAUFMANN and K. SCHENKER, *ibid.* **12** (1994) 203.
10. G. PAPAVASSILIOU, F. MILIA, M. FARDIS, R. RUMM, E. LAGANAS, O. JARH, A. SEPE, R. BLINC and M. M. PINTAR, *J. Amer. Ceram. Soc.* **76** (1993) 2109.
11. J. J. ATTARD, S. J. DORAN, N. J. HERROD, T. A. CARPENTER and L. D. HALL, *J. Magn. Reson.* **96** (1992) 514.
12. J. L. A. WILLIAMS, D. G. TAYLOR, G. MADDINELLI, P. ENWERE and J. S. ARCHER, *Magn. Reson. Imaging* **9** (1991) 767.
13. L. D. HALL and V. RAJANAYAGAM, *J. Magn. Reson.* **74** (1987) 139.
14. P. JEZZARD, J. J. ATTARD, T. A. CARPENTER and L. D. HALL, *Prog. NMR Spect.* **23** (1991) 1.
15. D. G. CORY, *Annu. Rep. NMR Spectrosc.* **24** (1992) 87.
16. S. J. BLACK, D. M. LANE, P. J. McDONALD, D. J. HANNANT, M. J. MULHERON, G. HUNTER and M. R. JONES, *J. Mater. Sci. Lett.* **14** (1995) 1175.
17. T. NUNES, E. W. RANDALL, A. A. SAMOILENKO, P. BODART and G. FEIO, in press.
18. P. J. McDONALD, T. PRITCHARD and S. P. ROBERTS, *J. Coll. and Int. Sci.* **177** (1996) 439.
19. S. P. COTTRELL, M. R. HALSE and J. H. STRANGE, *Meas. Sci. Technol.* **1** (1990) 624.
20. T. B. BENSON and P. J. McDONALD, *Physica B* **192** (1993) 269.
21. S. MEIBOOM and D. GILL, *Rev. Sci. Instrum.* **29** (1958) 688.
22. S. O. N. NWAUBANI, M. MULHERON and J. DUMBELTON, "Retreatment of Consolidated Stone faces–Appraisal of Existing Test methods", EC Contract No. EV5V-CT94-0518 (1995).
23. S. P. ROBERTS, P. J. McDONALD and T. PRITCHARD, *J. Magn. Reson.* **A116** (1995) 189.

Received 23 April
and accepted 21 May 1996